



Gemcitabine Enhances Kras-MEK-Induced Matrix Metalloproteinase-10 Expression Via Histone Acetylation in Gemcitabine-Resistant Pancreatic Tumor-initiating Cells

Shimizu, Kazuya
Nishiyama, Takaaki
Hori, Yuichi

(Citation)

Pancreas, 46(2) :268-275

(Issue Date)

2017-02

(Resource Type)

journal article

(Version)

Accepted Manuscript

(Rights)

© 2017 Wolters Kluwer Health. This is a non-final version of an article published in final form in Pancreas 46(2), 268-275, 2017

(URL)

<https://hdl.handle.net/20.500.14094/90003773>



Gemcitabine Enhances Kras-MEK-induced Matrix Metalloproteinase-10 Expression via Histone Acetylation in Gemcitabine-resistant Pancreatic Tumor-initiating Cells

Kazuya Shimizu, MD, PhD^{1,2}, Takaaki Nishiyama, MSc², and Yuichi Hori, MD, PhD²

¹Department of Internal Medicine, Kobe Medical Center; ²Division of Medical
Chemistry, Department of Biophysics, Kobe University Graduate School of Health
Sciences, Kobe, Japan

Correspondence: Yuichi Hori, MD, PhD, Division of Medical Chemistry, Department
of Biophysics, Kobe University Graduate School of Health Sciences, Tomogaoka
7-10-2, Suma-ku, Kobe, 654-0142, Japan

Phone: +81-78-796-4540; **Fax:** +81-78-796-4540; **E-mail:** horiy@people.kobe-u.ac.jp

Running title: Synergistic effect of Kras^{G12V} with Gemcitabine

Key Words: gemcitabine, Kras, MMP-10, histone acetylation, pancreatic
tumor-initiating cell

Funding: this study was supported by Grants-in-Aid for Scientific Research from The Ministry of Education, Culture, Sports, Science and Technology of Japan to K.S. (26462059) and Y.H. (15K10183).

Disclosure Statement: the authors have no conflict of interest.

ABSTRACT:

Objectives: Advanced pancreatic ductal adenocarcinoma is resistant to systemic chemotherapy, resulting in a poor prognosis. We previously isolated a human pancreatic tumor-initiating cell line, KMC07, from a patient with acquired resistance to gemcitabine chemotherapy. To improve the anti-cancer effects of gemcitabine, we investigated the molecular mechanism of KMC07 cells' resistance to gemcitabine.

Methods: KMC07 cells were treated with gemcitabine, then gene expression and functional analyses performed using microarray, the quantitative polymerase chain reaction, immunoblotting, immunohistochemistry, chromatin immunoprecipitation, and cell transplantation into nude mice.

Results: KMC07 cells, but not BxPC-3, PANC-1, MIAPaCa-2 or AsPC-1 cells, expressed *matrix metalloproteinase-10* mRNA, the expression level of which was enhanced by gemcitabine. KMC07 cells were shown to carry a constitutively active Kras mutation, and a MEK inhibitor suppressed *matrix metalloproteinase-10* mRNA expression. Gemcitabine enhanced histone H3 acetylation at the *matrix metalloproteinase-10* promoter, and a histone acetyltransferase inhibitor reduced

gemcitabine-enhanced *matrix metalloproteinase-10* mRNA expression. Gemcitabine induced expression of matrix metalloproteinase-10 protein in KMC07-derived pancreatic tumors *in vivo*.

Conclusions: We demonstrated constitutive activation of the Kras -MEK-matrix metalloproteinase-10 signaling pathway in KMC07 cells that was enhanced by gemcitabine through histone acetylation. Our results may provide novel insights into gemcitabine-based treatment for gemcitabine-resistant pancreatic ductal adenocarcinoma.

INTRODUCTION

Pancreatic ductal adenocarcinoma (PDAC) is currently the fourth leading cause of cancer-related mortality. The nucleoside analogue, gemcitabine, is the established standard treatment choice for advanced PDAC.¹ The FOLFIRINOX treatment protocol (folic acid, fluorouracil, irinotecan, and oxaliplatin) results in an improved overall survival of 11.1 months, compared to 6.8 months in controls using gemcitabine alone,²

but requires carefully selected patients with good performance status and the absence of several contraindications. Therefore, gemcitabine remains a key drug for treatment,^{3,4} and clarifying the molecular mechanisms related to gemcitabine resistance is important for improving treatment and increasing overall survival.

Kras with a constitutively active (CA) mutation is found in almost 95% of PDAC cases.^{5,6} In model systems, the Kras CA mutation induces formation of premalignant lesions in the pancreas, and in combination with a p53 mutation or chronic inflammation, is able to induce PDAC.⁷⁻⁹ Because the Kras CA mutation plays a pivotal role in formation of PDAC, small molecular inhibitors targeting Kras signaling molecules have been developed.¹⁰ Their recent clinical application has, however, highlighted that many of these inhibitors activate resistance-causing feedback mechanisms and are a cause for concern regarding their toxicity in the clinic.⁴

Extracellular matrix-related proteins are involved in proliferation and metastasis of PDAC.¹¹⁻¹⁵ Matrix metalloproteinase-10 (MMP-10) expression is induced in pancreatic cancer and its inhibition results in suppression of metastasis and invasion.¹⁶ MMP-10 expression is regulated by Kras signaling in lung cancer stem cells

¹⁷ and by histone acetylation in vascular endothelial cells.¹⁸ However, the molecular mechanisms involving MMP-10 that underly gemcitabine-resistant PDAC remain unclear.

We previously isolated gemcitabine-resistant pancreatic tumor-initiating cell lines, KMC cell lines, from advanced PDAC patients who were resistant to gemcitabine chemotherapy.¹⁹ In this study, we examined molecular mechanisms of gemcitabine resistance using one of these cell lines, KMC07.

MATERIALS AND METHODS

KMC07, Stromal, and Pancreatic Cancer Cell Lines

The human pancreatic tumor-initiating cell line KMC07 was isolated from a gemcitabine-resistant PDAC patient.¹⁹ The mouse stromal cell line PA6 (a gift from Dr. Nishikawa [RIKEN, Kobe, Japan]) was maintained in α -minimum essential medium (Invitrogen, Carlsbad, CA) containing 10% fetal calf serum.²⁰ KMC07 cells were co-cultured with PA6 cells in serum-free Stem medium (catalog number DSRK100, DS

Pharma Biomedical, Osaka, Japan) containing 0.1 μ M 2-mercaptoethanol, 50 U/ml of penicillin, and 50 μ g/ml of streptomycin (Thermo Fisher Scientific Inc., Rockford, IL, USA) at 37°C in a humidified atmosphere containing 5% CO₂. Human pancreatic cancer cell lines: BxPC-3, PANC-1, MIAPaCa-2, and AsPC-1 cells, were obtained from American Type Culture Collection (Rockville, MD, USA).

Engraftment of KMC07 Cells

Approximately 8 week-old male nude mice (BALB/cAJcl-nu/nu) (CLEA, Tokyo, Japan) were used. All nude mice were housed and used under the approved protocols in accordance with the Kobe University guidelines for the care and use of laboratory animals (Permit Number: A120905). KMC07 cells co-cultured with PA6 cells were harvested, dissociated and suspended in 1 ml of PBS. Nonspecific antibody binding was blocked using purified rat anti-mouse CD16/CD32 monoclonal antibodies (BD Biosciences, San Jose, CA, USA) and a human FcR blocking reagent (Miltenyi Biotech, Bergisch Gladbach, Germany) for 15 minutes on ice. KMC07 cells, after blocking, were separated from mouse PA6 cells expressing mouse PDGFR β by MACS Separator (Miltenyi Biotech) using a biotin-conjugated anti-mouse PDGFR β

monoclonal antibody (eBioscience, San Diego, CA, USA) and anti-biotin Microbeads (Miltenyi Biotech) according to manufacturers' protocols. Purities ranged from 95 to 98% for each cell population, evaluated by FACS analyses (data not shown). After a small left abdominal flank incision was made, 200 μ L of the separated KMC07 cells (1×10^6 KMC07 cells in 200 μ L of serum-free Stem medium) was injected in a region of the pancreas tail using a 1 mL disposable syringe attached to a 30-gauge needle (TERUMO, Tokyo, Japan). One layer of the abdominal wound was closed with an Auto-clip (Clay Adams, Parsippany, NJ, USA). After 8 weeks, the mice were sacrificed under anesthesia. Tissue samples were fixed in 10% phosphate-buffered formalin overnight and embedded in paraffin. For gemcitabine treatment, 8 weeks after injection of KMC07 cells into subcutaneous fat or a region of the pancreas tail, 120 mg/kg of gemcitabine (Eli Lilly Japan KK, Tokyo, Japan) or saline, for controls, was injected intraperitoneally, twice a week for 4 weeks. The mice were then sacrificed under anesthesia. Tissue samples were fixed in 10% phosphate-buffered formalin overnight and embedded in paraffin.

Immunohistochemistry

Immunohistochemical staining was performed as described previously.²¹

Immunostaining to detect MMP-10 expression in human tissues was performed on 3- μ m sections from formalin-fixed, paraffin-embedded tissues, placed on coated glass slides, and dried at room temperature overnight. Sections were dewaxed in xylene and rehydrated according to standard procedures. For antigen retrieval, the tissue sections were boiled in 1 \times Target Retrieval Solution pH 9.0 (Dako, Carpinteria, CA, USA) for 40 minutes. The samples were cooled at room temperature for 20 minutes and rinsed with distilled water 3 times, followed by peroxidase block with 3% H₂O₂ in methanol for 5 minutes. After rinsing twice with distilled water, the samples were immersed in Tris-buffered saline-Tween20 (TBST) (25 mM Tris-HCl [pH 7.4], 75 mM NaCl, and 0.1% Tween20) for 5 minutes and then incubated with a primary antibody (a rabbit anti-human MMP-10 polyclonal antibody (catalog number PA5-29746, Thermo Fisher Scientific Inc.) diluted 1:250 in Dako Real antibody diluent (catalog number S202230, Dako, Burlington, ON, Canada) at 4°C overnight. The samples were rinsed 3 times with TBST. The primary antibody detection was performed with rabbit horseradish peroxidase polymer probe (ChemMate™ DAKO EnVision™ Detection Kit,

Peroxidase/DAB, Rabbit, catalog number K5007, Dako) at room temperature for 30 minutes, followed by two rinses with TBST according to the manufacturer's instructions. The signal was developed with diaminobenzidine (Dako) for 10 minutes. The samples were rinsed with distilled water 3 times, counterstained with hematoxylin for 1 minute, and dehydrated in alcohol solution and xylene. Parallel sections were stained with hematoxylin and eosin for identification of cancerous and normal tissues.

Microarrays

KMC07 cells co-cultured with PA6 cells in a 10-cm Corning[®] culture dish (Corning, Corning, NY, USA) were incubated with 2 μ M gemcitabine or phosphate-buffered saline (PBS). After 48 hours, RNAs were extracted using an RNAeasy mini kit (Qiagen, Venlo, Netherland),²² and subjected to microarray analyses as described.²³

Reverse Transcription (RT)-Polymerase Chain Reaction (PCR) and Quantitative

Real Time (qRT)-PCR Assays

RT-PCR was performed as described.²³ qRT-PCR was performed with a QuantiTect SYBR[®] Green RT-PCR kit (catalog number 204243, Qiagen) using the

Applied Biosystems 7500 Real-Time PCR System (Life Technologies, Carlsbad, CA, USA) according to manufacturers' protocols.¹⁹ Quantification of *MMP10* mRNA expression was determined by the relative standard curve method with *human β-actin* as an endogenous control. The amount of *MMP10* promoter genomic DNA immunoprecipitated in ChIP assays was quantified using PCR. The primer sequences used were:

human-*β-actin*-F/104: 5'-AGCCTCGCCTTTGCCGATCC-3'

human-*β-actin*-R/104: 5'-TTGCACATGCCGGAGCCGTT-3'

human-MMP-10-F/119: 5'-AGTTTGGCTCATGCCTACCC-3'

human-MMP-10-R/119: 5'-TCATGAGCAGCAACGAGGAA-3'

human-MMP-2-F/222: 5'-CCGCCTTTAACTGGAGCAAA-3'

human-MMP-2-R/222: 5'-TTTGGTTCTCCAGCTTCAGG-3'

human- MMP-10 promoter-F/149: 5'-ACCAAGCTTGTCAGCTCTCTTT-3'

human- MMP-10 promoter-R/149: 5'-CAGCCTACATCAGTATTTTCCTTCA-3'

Kras Mutation Analyses

Kras and Nras mutations (codon: 12, 13, 59, 61, 117, 146) were analyzed by

the PCR-reverse sequence specific oligonucleotide (PCR-rSSO) method as described.²⁴

Briefly, genomic DNA was obtained from xenograft tumor tissue samples. Tissue samples were fixed in 10% phosphate-buffered formalin overnight and embedded in paraffin. Ten- μ m sections were prepared using formalin-fixed, paraffin-embedded tissues, placed on coated glass slides, and dried at room temperature overnight. The samples were sent to the research institution (SRL, Tokyo, Japan). Genomic DNA was isolated from the samples and 50 ng of template DNA was amplified by PCR using a biotin-labeled primer. The PCR products and fluorescent beads (oligonucleotide probes complementary to wild and mutant genes were bound to the beads) were hybridized and labeled with streptavidin-phycoerythrin. The products were subjected to PCR-rSSO assays and collected data were analyzed using UniMAG software (MBL, Nagoya, Japan).

Immunoblotting

KMC07 cells, co-cultured with PA6 cells in a 6-well CostarTM cell culture plate (Thermo Fisher Scientific Inc.), were treated with 0.125 μ M gemcitabine for 48 hours. Cells were washed twice with 3 ml of ice-cold PBS and resuspended with 200 μ L

of Laemmli sample loading buffer (2% SDS, 20 mM DTT, 10% glycerol, 62.5 mM Tris-HCl [pH 6.8], and 0.002% bromophenol blue). The samples were sonicated for 10 seconds and boiled for 5 minutes. The samples were subjected to SDS-PAGE, along with molecular weight markers, Precision Plus Protein™ Standards Unstained Protein Standards (catalog number 161-0363, Bio-Rad, Hercules, CA, USA) and Precision Plus Protein™ Kaleidoscope™ Standards (catalog number 161-0375, Bio-Rad), using e-PAGEL 5%-20% gel (catalog number E-T520L, ATTO, Tokyo, Japan). Proteins were transferred from the gel to a nitrocellulose membrane (iBlot® gel Transfer Stacks Nitrocellulose, Mini, Thermo Fisher Scientific Inc.) for 7 minutes using the iBlot™ Gel Transfer System (catalog number IB1001, Invitrogen, Carlsbad, CA) according to manufacturers' protocols. The blotted membrane was rinsed with PBS for 5 minutes, and blocked with 5% skim milk in TBST at room temperature for 1 hour. The membrane was washed 3 times with 25 ml of TBST for 5 minutes and incubated with a primary antibody (a rabbit anti-human MMP-10 polyclonal antibody diluted 1:100 in 5% bovine serum albumin (BSA) in TBST) at 4°C overnight. The membrane was rinsed 3 times with TBST for 5 minutes, and incubated with a secondary antibody (an HRP

conjugated goat anti-rabbit IgG [H+L] (catalog number G-21234, Thermo Fisher Scientific Inc.) diluted 1:20,000 in TBST with 5% BSA) and StrepTactin-HRP conjugate (catalog number 161-0382, Bio-Rad) diluted 1:20,000 in TBST with 5% BSA at room temperature for 1 hour. The membrane was rinsed 5 times with TBST for 5 minutes, and incubated with the SuperSignal West Dura Extended Duration Substrate (catalog number 34075, Thermo Fisher Scientific Inc.) according to a manufacturer's protocol. The chemiluminescent signals were captured using a CCD camera-based imager (Optima Shot CL-420 α , Wako Pure Chemical Industries, Osaka, Japan) and analyzed using software (Basic QuantifierTM v.3.3.5, Bio Image Systems Inc., Tokyo, Japan). To detect human CoxIV (3E11) protein as an endogenous control, the blotted membrane was incubated with an HRP-conjugated rabbit anti-human CoxIV monoclonal antibody (catalog number 5247, Cell Signaling Technology, Danvers, MA, USA) diluted 1:1000 in TBST with 5% BSA in at room temperature for 1 hour.

Chromatin Immunoprecipitation (ChIP) Analyses

ChIP assays were performed using the Acetyl-Histone H3 Immunoprecipitation (ChIP) Assay Kit (catalog number 17-245, Millipore Corp.,

Billerica, MA, USA) according to a manufacturer's protocol. Briefly, KMC07 cells were co-cultured with PA6 cells with 4 ml of Stem medium in a 10-cm Corning® culture dish and treated with 0.125 μ M gemcitabine or PBS for 48 hours. One ml of 10% formalin solution (catalog number 060-03845, Wako Pure Chemical Industries) was added to each dish and cells were incubated at 37°C for 10 minutes. Cells were washed twice with 5 ml of ice-cold PBS with a protease inhibitor cocktail (cOmplete, catalog number 11697498001, Roche Diagnostics, Basel, Switzerland) on ice, harvested using a cell scraper (catalog number 9000-220, AGC Techno Glass Co., Ltd., Shizuoka, Japan) into a 1.5-ml conical tube, and pelleted by a centrifugation at 2,000 X G at 4°C for 4 minutes. Cells (approximately 1×10^6 cells) were re-suspended in 200 μ L of SDS Lysis Buffer (catalog number 20-163, Millipore) with a protease inhibitor cocktail and incubated for 10 minutes on ice. The lysate was sonicated 6 times using an Ultrasonic Disrupter (Handy Sonic UR-20P, TOMY, Tokyo, Japan) at 20 Watts for 30 seconds on ice (at 5-minute intervals). The samples were centrifuged at 21,500 X G at 4°C for 10 minutes, and the supernatants were transferred into a 2-ml conical tube and diluted with 1800 μ l of CHIP Dilution Buffer (catalog number 20-153, Millipore). A 200 μ l aliquot

of the diluted sample was transferred to another tube as an “In-put sample”. The remaining samples were incubated with 75- μ l Salmon Sperm DNA/Protein A Agarose-50% Slurry (catalog number 16-157, Millipore) at 4°C for 30 minutes with rotation and centrifuged at 1,000 X G at 4°C for 1 minute. The supernatant was transferred to a conical tube and incubated with 4 μ l of a rabbit anti-acetyl-Histone H3 polyclonal antibody (catalog number 06-599, Millipore) at 4°C overnight with constant rotation. Sixty μ l of Salmon Sperm DNA/Protein A Agarose-50% Slurry was added to the conical tube and incubated at 4°C for 1 hour with constant rotation. After centrifugation at 1,000 X G at 4°C for 1 minute, the supernatant was removed and the Protein A agarose was sequentially washed with Low Salt Immune Complex Wash Buffer (catalog number 20-154, Millipore), High Salt Immune Complex Wash Buffer (catalog number 20-155, Millipore), LiCl Immune Complex Wash Buffer (catalog number 20-156, Millipore), and TE Buffer (catalog number 20-157, Millipore) at 4°C. The Protein A agarose was incubated with 250 μ l of elution buffer (1% SDS and 0.1 M NaHCO₃) for 15 minutes and centrifuged at 1,000 X G for 1 minute at room temperature. The supernatant was transferred to another tube, and this elution procedure

was repeated. The combined supernatant (total 500 μ l), “Elution sample”, and “In-put sample” (total 200 μ l) were mixed with 5 M NaCl (final concentration, 0.2 M) and incubated at 65°C for 4 hours. After incubation, the samples were mixed with reaction buffer (final concentration: 36 mM Tris-HCl (pH6.5), 18 mM EDTA, 0.18 M NaCl, and 0.36 g/L Proteinase K (catalog number MC5005, Promega, Madison, WI, USA)), and incubated further at 45°C for 1 hour. The samples were treated with an equal volume of Phenol: Chloroform: Isoamyl Alcohol Mixed, pH 7.9 (catalog number 25970-14, Nacalai Tesque, Kyoto, Japan) and precipitated with ethanol and linear polyacrylamide prepared as described.²⁵ The precipitates were washed with 70% ethanol and dissolved in 20 μ l of DNase-free water, followed by qRT-PCR using *human MMP-10* promoter primers.

Statistical Analyses

Results for continuous variables were expressed as the mean \pm standard error (SE). Statistically significant differences were determined by the Student's *t*-Test. Significance was defined as *, $p < 0.05$.

This study was performed according to Institutional Review Board-approved guidelines in Kobe Medical Center and Kobe University School of Health Sciences and approved by the Ethics Committees of Kobe Medical Center and Kobe University School of Health Sciences (permission No.152).

RESULTS

***MMP-10* mRNA Expression was Up-regulated by Gemcitabine in KMC07 Cells**

We previously isolated and characterized seven pancreatic tumor-initiating cell lines from 7 independent PDAC patients who were resistant to gemcitabine treatment.¹⁹ The KMC07 patient was treated with gemcitabine for three years. His liver metastases disappeared and his pancreatic tumor became smaller (partial response) for the first two years of treatment. After the partial response, the liver metastases slowly recurred, accompanied by peritoneal dissemination for the last year of treatment (Fig. 1A). The KMC07 cell line was derived from the KMC07 patient, suggesting that KMC07 cells might have acquired, or congenitally possess, gemcitabine resistance.

Engraftment of KMC07 cells into the pancreatic tail or subcutaneous fat of nude mice resulted in the formation of tumors, accompanied by liver and lung metastases (Fig. 1B). To identify genes in KMC07 cells that are upregulated in response to gemcitabine, KMC07 cells were treated with or without gemcitabine, then subjected to microarray analyses. We found that *MMP-10* was the most highly induced gene on the array, followed by *synaptotagmin XVI* and *transmembrane protein 40* (Fig. 1C).

In this study we characterized the interaction between *MMP-10* mRNA up-regulation and gemcitabine resistance. We examined *MMP-10* mRNA expression levels in KMC07 cells and the cultured pancreatic cancer cell lines: BXPc-3, MIAPaCa-2, PANC-1, and AsPC-1 cells. KMC07 cells, but none of the other cultured cell lines, expressed *MMP-10* mRNA, which was up-regulated upon gemcitabine treatment. KMC07 cells did not express *MMP-2* mRNA; a gene expressed by PANC-1 cells (Fig. 2A).²⁶ Gemcitabine up-regulated *MMP-10* mRNA expression in KMC07 cells in a dose-dependent manner (Fig. 2B). We also confirmed that gemcitabine up-regulated MMP-10 protein expression in KMC07 cells (Fig. 2C).

Up-regulation of Kras-MEK-induced *MMP-10* mRNA Expression by Gemcitabine

We confirmed that KMC07 cells expressed the Kras CA mutant, Kras^{G12V}, by the PCR-rSSO method (Fig. 3A). We asked if the Kras^{G12V} signaling pathway regulates gemcitabine-enhanced MMP-10 expression. A MEK inhibitor, U0126, reduced the basal level of *MMP-10* mRNA expression in KMC07 cells, in the absence of gemcitabine (Fig. 3B). Moreover, U0126 suppressed gemcitabine-enhanced expression of *MMP-10* mRNA (Fig. 3C). These results demonstrate that Kras^{G12V}-MEK signaling-induced expression of *MMP-10* mRNA is up-regulated by gemcitabine in KMC07 cells.

Requirement of Histone Acetylation for Gemcitabine-dependent *MMP-10* mRNA Expression

We examined whether histone acetylation was involved with gemcitabine-enhanced MMP-10 expression in KMC07 cells. Gemcitabine-enhanced *MMP-10* mRNA expression was reduced by C646, a histone acetyltransferase inhibitor (Fig. 4A). Trichostatin A (TSA), a histone deacetylase (HDAC) inhibitor, enhanced *MMP-10* mRNA expression, while C646 reduced TSA-enhanced *MMP-10* mRNA expression (Fig. 4B). TSA-enhanced *MMP-10* mRNA expression was reduced by U0126 (Fig. 4B). Gemcitabine exhibited enhanced histone H3 acetylation level at an

MMP-10 promoter in ChIP assays (Fig. 4C). These results demonstrate that histone acetylation is required for gemcitabine-induced up-regulation of *MMP-10* mRNA expression.

Induction of MMP-10 Protein Expression in KMC07-derived Tumor by Gemcitabine *in vivo*

Gemcitabine reduced the growth rate of KMC07-derived subcutaneous tumors in nude mice (Fig. 5A). To test whether gemcitabine up-regulated MMP-10 expression in KMC07-derived tumors, KMC07 cells were injected into a region of the pancreas tail of nude mice and gemcitabine subsequently administered intraperitoneally. The growth rate of KMC07-derived orthotopic pancreatic tumor was also reduced in the presence of gemcitabine (Fig. 5B). Histologically, gemcitabine enhanced the invasion of KMC07-derived tumor cells into normal pancreas tissues, and partially up-regulated MMP-10 expression, while in the absence of gemcitabine, KMC07-derived tumor cells grew expansively within the fibrous capsule (Fig. 5B). These results suggest that gemcitabine up-regulates MMP-10 protein expression in KMC07-derived orthotopic pancreatic tumors.

DISCUSSION

This is the first demonstration that the gemcitabine-enhanced Kras^{G12V}-MEK-MMP-10 signaling pathway was activated in gemcitabine-resistant PDAC *in vivo* and *in vitro*. This suggests that acquiring gemcitabine resistance may unlock the Kras^{G12V} signaling pathway that is inactivated in naïve PDAC.

The KMC07 cell line characterized in this study is one of 7 KMC cell lines that we have previously reported.¹⁹ The 6 other KMC cell lines also expressed *MMP-10* mRNA at levels similar to that of the KMC07 cell line in the absence of gemcitabine (data not shown). MMP-10 was required for invasion and metastasis of pancreatic cancer.¹⁶ MMP-10 cleaved collagen type-I in co-operation with MMP-1, resulting in re-organization of the extracellular matrix.²⁷ MMP-1 was also required for Kras CA mutant-regulated invasion of human pancreatic cancer cells via ERK2.²⁸ Taken together, these results suggest that KMC07 cells re-organize extracellular matrix through Kras^{G12V}-induced activation of MMP-10, followed by invasion and metastasis. MIAPaCa-2, PANC-1, and AsPC-1 cells, but not BxPC-3 cells express the Kras CA

mutant.²⁹ However, MIAPaCa-2, PANC-1, and AsPC-1 cells, did not express *MMP-10* mRNA. If presence of the Kras CA mutation was sufficient to induce *MMP-10* mRNA expression, these cultured cell lines would express *MMP-10* mRNA. Therefore, our results indicate that a Kras CA mutation is necessary, but not sufficient for *MMP-10* induction, and that other unknown factors might be required for Kras CA mutant-MEK-dependent induction of *MMP-10*.

A low level of histone acetylation in pancreatic cancer is a predictor of poor survival³⁰ and HDAC inhibitors are currently being evaluated in trials.^{31,32} In contrast, we showed that gemcitabine enhanced histone H3 acetylation levels at an *MMP-10* promoter, and that this was reduced by a histone acetyltransferase inhibitor. Moreover, TSA enhanced the *MMP-10* mRNA expression level in KMC07 cells, consistent with a previous report that HDAC-7 repressed *MMP-10* gene transcription by associating with myocyte enhancer factor-2.¹⁸ Another group recently showed that gemcitabine treatment increased histone acetylation levels at a pro-oncogenic molecule *miR-21* promoter in cultured pancreatic cancer cell lines.^{33,34} Taken together, these results suggest that the effects of histone acetylation on PDAC may be context-dependent. It remains unknown

how gemcitabine increases histone H3 acetylation levels at the *MMP-10* promoter, however, it is possible that gemcitabine blocks DNA replication and leads to a DNA damage response that includes acetylation of histones in a context-dependent manner.^{35,36}

We showed that gemcitabine-enhanced MMP-10 expression was completely inhibited by a MEK inhibitor, U0126.³⁷ A Notch inhibitor, DAPT,³⁸ and a TGF- β receptor antagonist, SB431542,³⁹ partially reduced gemcitabine-enhanced *MMP-10* mRNA expression (data not shown). Therefore, the Kras^{G12V}-MEK signaling pathway is necessary for MMP-10 expression, and Notch and TGF- β signals might function as enhancers for MMP-10 expression.

To improve the anti-cancer effects of gemcitabine on PDAC, molecular mechanisms of gemcitabine resistance are under intense investigation.³ Our results demonstrate a unique gemcitabine-resistance mechanism using novel pancreatic tumor-initiating cells, and suggest that not only MMP-10, but also other cancer-related genes downstream of Kras^{G12V} signaling pathways, may be activated when PDAC becomes resistant to gemcitabine. It is possible that a combination of gemcitabine and

MEK inhibitors, as well as MMP-10 inhibitors, might synergistically improve the overall survival of gemcitabine-resistant PDAC patients.

ACKNOWLEDGEMENT

The authors thank Dr. Fiona Stennard for her proofreading and critical comments on this manuscript.

REFERENCES

1. Burris HA, Moore MJ, Andersen J, et al. Improvements in survival and clinical benefit with gemcitabine as first-line therapy for patients with advanced pancreas cancer: a randomized trial. *J Clin Oncol*. 1997;15:2403–2413.
2. Conroy T, Desseigne F, Ychou M, et al. FOLFIRINOX versus gemcitabine for metastatic pancreatic cancer. *N Engl J Med*. 2011;364:1817–1825.
3. de Sousa Cavalcante L, Monteiro G. Gemcitabine: Metabolism and molecular mechanisms of action, sensitivity and chemoresistance in pancreatic cancer. *Eur J Pharmacol*. 2014;741:8–16.
4. Michl P, Gress T. Current concepts and novel targets in advanced pancreatic cancer. *Gut*. 2013;62:317–326.
5. Jaffee EM, Hruban RH, Canto M, et al. Focus on pancreas cancer. *Cancer Cell*. 2002;2:25–28.
6. Hidalgo M. Pancreatic Cancer. *N Engl J Med*. 2010;362:1605–1617.
7. Hatzivassiliou G, Haling JR, Chen H, et al. Mechanism of MEK inhibition determines efficacy in mutant KRAS- versus BRAF-driven cancers. *Nature*.

2013;501:232–236.

8. von Karstedt S, Conti A, Nobis M, et al. Cancer Cell-autonomous TRAIL-R signaling promotes KRAS-driven cancer progression, invasion, and metastasis. *Cancer Cell*. 2015;27:561–573.
9. Hingorani SR, Petricoin EF, Maitra A, et al. Preinvasive and invasive ductal pancreatic cancer and its early detection in the mouse. *Cancer Cell*. 2003;4:437–450.
10. Baines AT, Xu D, Der CJ. Inhibition of Ras for cancer treatment: the search continues. *Future Med Chem*. 2011;3:1787–1808.
11. Zhao X, Gao S, Ren H, et al. Hypoxia-inducible factor-1 promotes pancreatic ductal adenocarcinoma invasion and metastasis by activating transcription of the actin-bundling protein fascin. *Cancer Res*. 2014;74:2455–2464.
12. Aguilera KY, Rivera LB, Hur H, et al. Collagen signaling enhances tumor progression after anti-VEGF therapy in a murine model of pancreatic ductal adenocarcinoma. *Cancer Res*. 2014;74:1032–1044.
13. Özdemir BC, Pentcheva-Hoang T, Carstens JL, et al. Depletion of

- carcinoma-associated fibroblasts and fibrosis induces immunosuppression and accelerates pancreas cancer with reduced survival. *Cancer Cell* 2014;25:719–734.
14. Rhim AD, Oberstein PE, Thomas DH, et al. Stromal elements act to restrain, rather than support, pancreatic ductal adenocarcinoma. *Cancer Cell*. 2014;25:735–747.
 15. Schlomann U, Koller G, Conrad C, et al. ADAM8 as a drug target in pancreatic cancer. *Nat Commun*. 2015;6:6175.
 16. Zhang JJ, Zhu Y, Xie KL, et al. Yin Yang-1 suppresses invasion and metastasis of pancreatic ductal adenocarcinoma by downregulating MMP10 in a MUC4/ErbB2/p38/MEF2C-dependent mechanism. *Mol Cancer*. 2014;13:130.
 17. Regala RP, Justilien V, Walsh MP, et al. Matrix metalloproteinase-10 promotes Kras-mediated bronchio-alveolar stem cell expansion and lung cancer formation. *PLoS One*. 2011;6:e26439.
 18. Chang S, Young BD, Li S, et al. Histone deacetylase 7 maintains vascular integrity by repressing Matrix Metalloproteinase 10. *Cell*. 2006;126:321–334.
 19. Shimizu K, Chiba S, Hori Y. Identification of a novel subpopulation of tumor-initiating cells from gemcitabine-resistant pancreatic ductal

- adenocarcinoma patients. *PLoS One*. 2013;8:e1–13.
20. Nishikawa S, Ogawa M, Nishikawa S, et al. lymphopoiesis on stromal cell clone: stromal cell clones acting on different stages of B cell differentiation. *Eur J Immunol*. 1988;18:1767–1771.
21. Shimizu K, Itoh T, Shimizu M, et al. CD133 expression pattern distinguishes intraductal papillary mucinous neoplasms from ductal adenocarcinomas of the pancreas. *Pancreas*. 2009;38:e207–e214.
22. Hori Y, Rulifson IC, Tsai BC, et al. Growth inhibitors promote differentiation of insulin-producing tissue from embryonic stem cells. *Proc Natl Acad Sci U S A*. 2002;99:16105–16110.
23. Hori Y, Fukumoto M, Kuroda Y. Enrichment of putative pancreatic progenitor cells from mice by sorting for prominin1 (CD133) and platelet-derived growth factor receptor β . *Stem Cells*. 2008;26:2912–2920.
24. Bando H, Yoshino T, Shinozaki E, et al. Simultaneous identification of 36 mutations in KRAS codons 61 and 146, BRAF, NRAS, and PIK3CA in a single reaction by multiplex assay kit. *BMC Cancer*. 2013;13:405.

25. Gaillard C, Strauss F, Monod IJ, et al. Ethanol precipitation of DNA with linear polyacrylamide carrier. *Nucleic Acids Res.* 1990;18:378.
26. Zervos EE, Shafii AE, Haq M, et al. Matrix metalloproteinase inhibition suppresses MMP-2 activity and activation of PANC-1 cells in vitro. *J Surg Res.* 1999;167:162–167.
27. Saunders WB, Bayless KJ, Davis GE. MMP-1 activation by serine proteases and MMP-10 induces human capillary tubular network collapse and regression in 3D collagen matrices. *J Cell Sci.* 2005;118:2325–2340.
28. Botta GP, Reginato MJ, Reichert M, et al. Constitutive K-Ras G12D activation of ERK2 specifically regulates 3D invasion of human pancreatic cancer. *Mol Cancer Res.* 2012;10:183–197.
29. Aoki K, Yoshida T, Matsumoto N, et al. Suppression of Ki-ras p21 levels leading to growth inhibition of pancreatic cancer cell lines with Ki-ras mutation but not those without Ki-ras mutation. *Mol Carcinog.* 1997;20:251–258.
30. Manuyakorn A, Paulus R, Farrell J, et al. Cellular histone modification patterns predict prognosis and treatment response in resectable pancreatic adenocarcinoma:

Results from RTOG 9704. *J Clin Oncol*. 2010;28:1358–1365.

31. Koutsounas I, Giaginis C, Patsouris E, et al. Current evidence for histone deacetylase inhibitors in pancreatic cancer. *World J Gastroenterol*. 2013;19:813–28.
32. Marks PA, Breslow R. Dimethyl sulfoxide to vorinostat: development of this histone deacetylase inhibitor as an anticancer drug. *Nat Biotechnol*. 2007;25:84–90.
33. Song WF, Wang L, Huang WY, et al. MiR-21 upregulation induced by promoter zone histone acetylation is associated with chemoresistance to gemcitabine and enhanced malignancy of pancreatic cancer cells. *Asian Pac J Cancer Prev*. 2013;14:7529–7536.
34. Frampton AE, Castellano L, Colombo T, et al. MicroRNAs cooperatively inhibit a network of tumor suppressor genes to promote pancreatic tumor growth and progression. *Gastroenterology*. 2014;146:268–277.
35. Huen MS, Chen J. The DNA damage response pathways: at the crossroad of protein modifications. *Cell Res*. 2008;18:8–16.

36. Jackson S, Bartek J. The DNA-damage response in human biology and disease. *Nature*. 2009;461:1071–1078.
37. Gysin S, Lee S, Dean NM, et al. Pharmacologic inhibition of RAF-MEK-ERK signaling elicits pancreatic cancer cell cycle arrest through induced expression of p27 Kip1. *Cancer Res*. 2005;65:4870–4880.
38. McClements L, Yakkundi A, Papaspyropoulos A, et al. Targeting treatment-resistant breast cancer stem cells with FKBPL and its peptide derivative, AD-01, via the CD44 pathway. *Clin Cancer Res*. 2013;19:3881–3893.
39. Singha PK, Yeh I, Venkatachalam MA, et al. Transforming growth factor- β (TGF- β)-inducible gene TMEPAI converts TGF- β from a tumor suppressor to a tumor promoter in breast cancer. *Cancer Res*. 2010;70:6377–6383.

FIGURE LEGENDS

FIGURE 1. A. Clinical course of a KMC07 patient. (a-d) ^{18}F -fluorodeoxyglucose accumulation at the pancreatic head (**a, c**) and liver (**b, d**) imaged by positron emission

tomography at first admission (**a, b**) and after 24-months gemcitabine treatment (**c, d**). (**e**) A computed tomography image after 35-months gemcitabine treatment. Asterisks indicate liver metastases. An arrow indicates pancreatic head cancer. (**f**) The time course of carbohydrate antigen 19-9 (CA19-9) during gemcitabine treatment. CRT stands for chemoradiotherapy (total 50.4 gray radiation and 7 g/m² of 5-fluorouracil). A red cross indicates death of the patient. **B. Xenograft of KMC07 cells.** (**a**) KMC07-derived pancreatic and subcutaneous tumors. (**b**) Metastases to lung and liver. Arrows indicate metastases. (**c-e**) H-E stains of a pancreatic tumor (**c**), liver metastasis (**d**), and a subcutaneous tumor (**e**). Magnifications: x200. The results are representative of three independent experiments. **C. Microarrays.** KMC07 cells co-cultured with PA6 cells were treated with PBS (veh) and gemcitabine (GEM), and subjected to microarray analyses.

FIGURE 2. A. Expression of *human MMP-2* and *MMP-10* mRNAs. KMC07 cells, cultured pancreatic tumor cell lines (BxPC-3, MIAPaKa-2, PANC-1, and AsPC-1 cells), or medium alone (control) were co-cultured with PA6 cells, then subjected to

qRT-PCR analysis. *Human β -actin* mRNA was used as an internal control. KMC07(G+) indicates KMC07 cells incubated with 0.5 μ M gemcitabine for 48 hours. Results are representative of three independent experiments. **B. Gemcitabine-dose-dependent *MMP-10* mRNA expression.** KMC07 cells co-cultured with PA6 cells were treated with the indicated concentrations of gemcitabine for 48 hours, and analyzed by qRT-PCR. The mRNA expression level is indicated by the mean \pm SE from three experiments completed in triplicate. **C. Human *MMP-10* protein expression.** KMC07 cells were co-cultured with PA6 cells with or without 0.5 μ M gemcitabine for the indicated periods then immunoblotted using an anti-MMP-10 antibody. Human CoxIV was used as an internal control. The result is representative of three independent experiments.

FIGURE 3. A. Kras mutation analysis in KMC07 cells. Kras and Nras mutations were analyzed by the PCR-rSSO method. **B. Effects of a MEK inhibitor on human *MMP-10* mRNA expression.** KMC07 cells co-cultured with PA6 cells were treated with 10 μ M U0126, or DMSO as a control, then analyzed by qRT-PCR. Columns

indicate the mean \pm SE from three experiments completed in triplicate; *, $p < 0.05$. C.

Effects of a MEK inhibitor on gemcitabine-enhanced *human MMP-10* mRNA expression. KMC07 cells co-cultured with PA6 cells were treated with 0.125 μ M gemcitabine in the presence of the indicated concentrations of U0126, then analyzed by qRT-PCR. Columns indicate the mean \pm SE from three experiments completed in triplicate.

FIGURE 4. A. Effects of a histone acetyltransferase inhibitor on gemcitabine-enhanced *human MMP-10* mRNA expression. KMC07 cells co-cultured with PA6 cells were treated with 0.125 μ M gemcitabine in the presence of the indicated concentrations of C646, and analyzed by qRT-PCR. Columns indicate the mean \pm SE from three experiments completed in triplicate. **B. Effects of a histone acetyltransferase inhibitor and a MEK inhibitor on HDAC inhibitor-enhanced *human MMP-10* mRNA expression.** KMC07 cells co-cultured with PA6 cells were treated with 4 μ M TSA in the presence of indicated concentrations of C646 or U0126, and analyzed by qRT-PCR. Columns indicate the mean \pm SE from three experiments

completed in triplicate. **C. ChIP assays.** KMC07 cells co-cultured with PA6 cells were treated with 0.125 μ M gemcitabine and subjected to ChIP analysis using an anti-acetyl-Histone H3 antibody. Histone H3 acetylation levels at the *MMP-10* promoter, expressed as the ratio of Elution to In-put sample levels, were compared in the presence and absence of gemcitabine. Columns indicate the mean \pm SE from three experiments completed in triplicate.

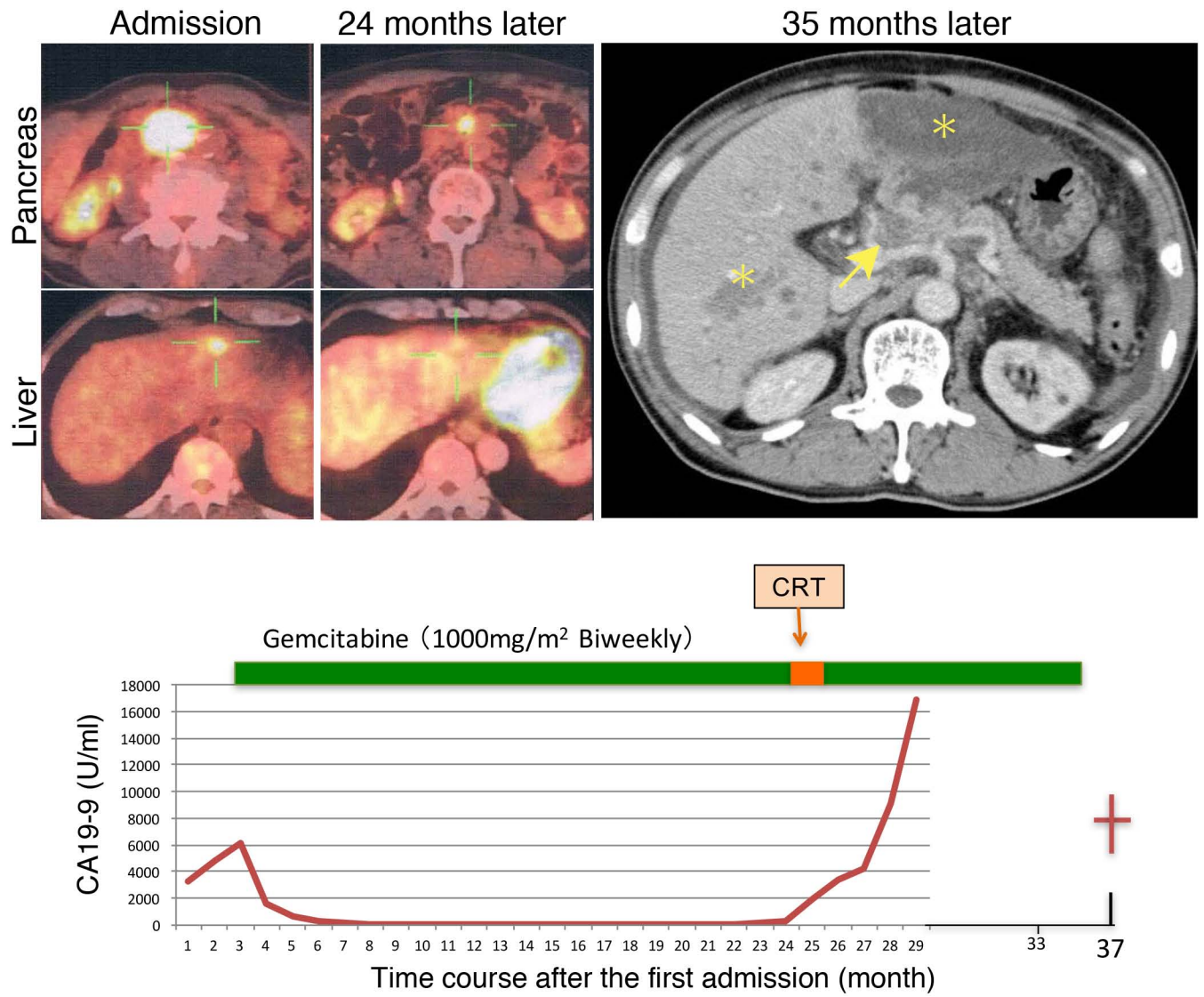
FIGURE 5. A. Reduction of the KMC07-derived tumor growth rate by gemcitabine. KMC07 cells were injected into the subcutaneous fat of nude mice. Mice were fostered for 8 weeks, by which time palpable tumors had formed underneath the skin. Gemcitabine, or saline as a control, was injected intraperitoneally twice a week for the indicated periods, and then tumor volume measured. The mean \pm SE from five experiments is shown; *, $p < 0.05$. **B. Up-regulation of human MMP-10 expression by gemcitabine in KMC07-derived pancreatic tumors.** Eight weeks after injection of KMC07 cells into a region of the pancreas tail, gemcitabine, or saline as a control, was injected intraperitoneally twice a week for 4 weeks. The resulting pancreatic tumors

were H-E stained and immunostained using an anti-human MMP-10 antibody.

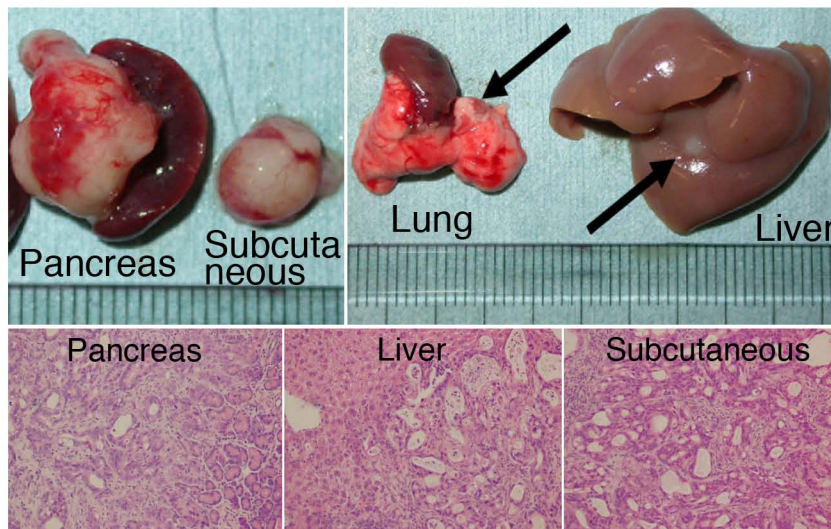
Arrowheads point to the pancreatic tumor. S, spleen; T, KMC07-derived tumor; and N,

normal pancreas region. Data are representative of three independent experiments.

A



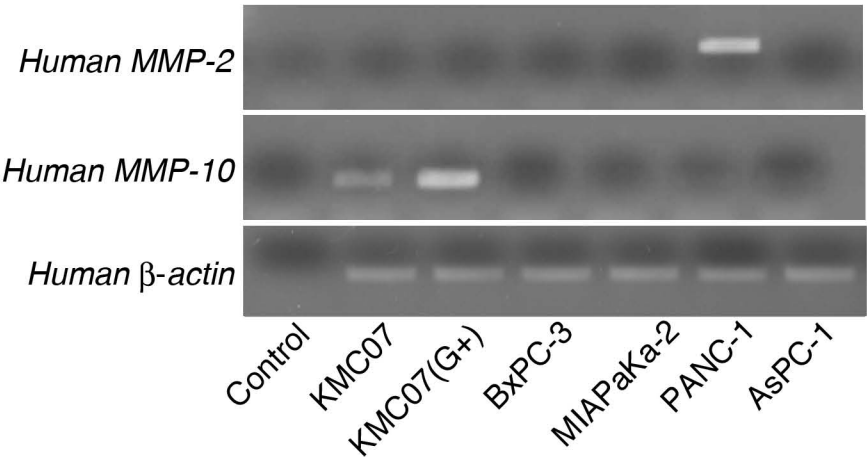
B



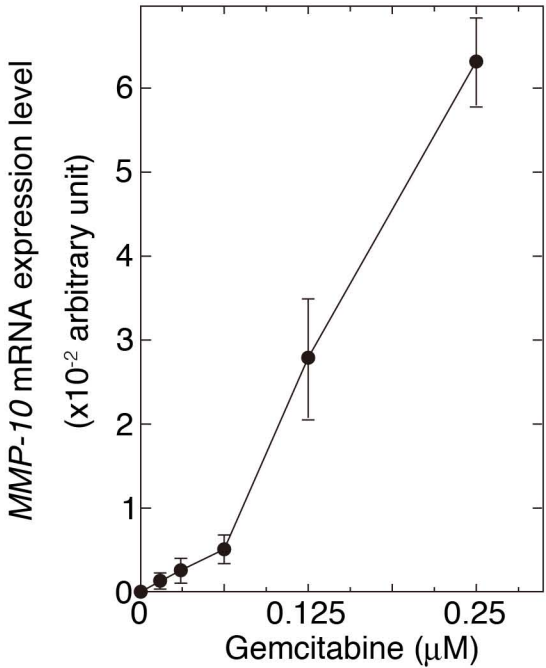
C

Signal (log2)		Average (log2)		Annotations	
KMC7_Veh	KMC7_GEM	KMC7-GEM_Veh		GeneSymbol	GeneName
5.0	12.7	7.7		MMP-10	matrix metalloproteinase 10
1.7	8.6	6.9		SYT16	synaptotagmin XVI
7.7	13.9	6.2		TMEM40	transmembrane protein 40

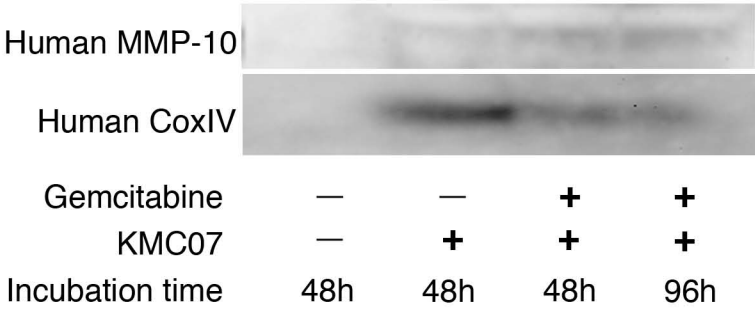
A



B



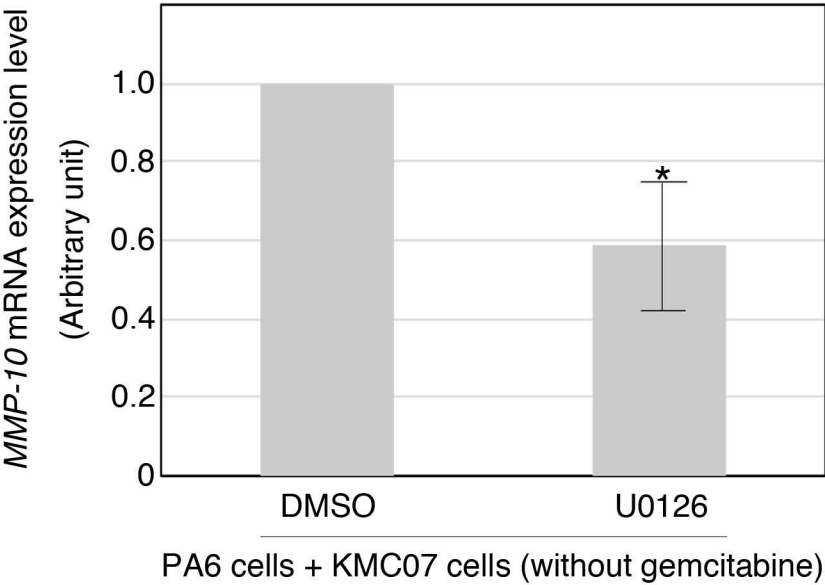
C



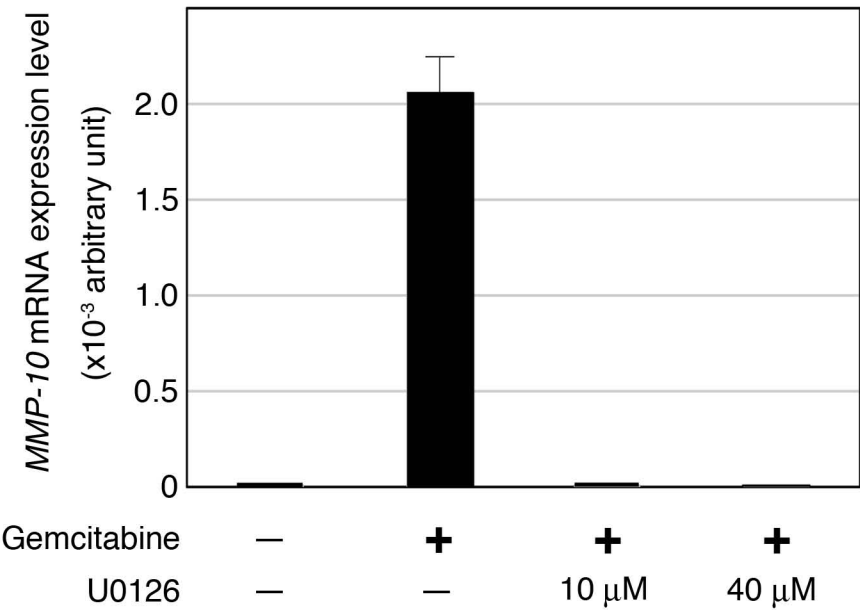
A

	Mutation		Mutation
Kras codon12	G12V	Nras codon12	none
Kras codon13	none	Nras codon13	none
Kras codon59	none	Nras codon59	none
Kras codon61	none	Nras codon61	none
Kras codon117	none	Nras codon117	none
Kras codon146	none	Nras codon146	none

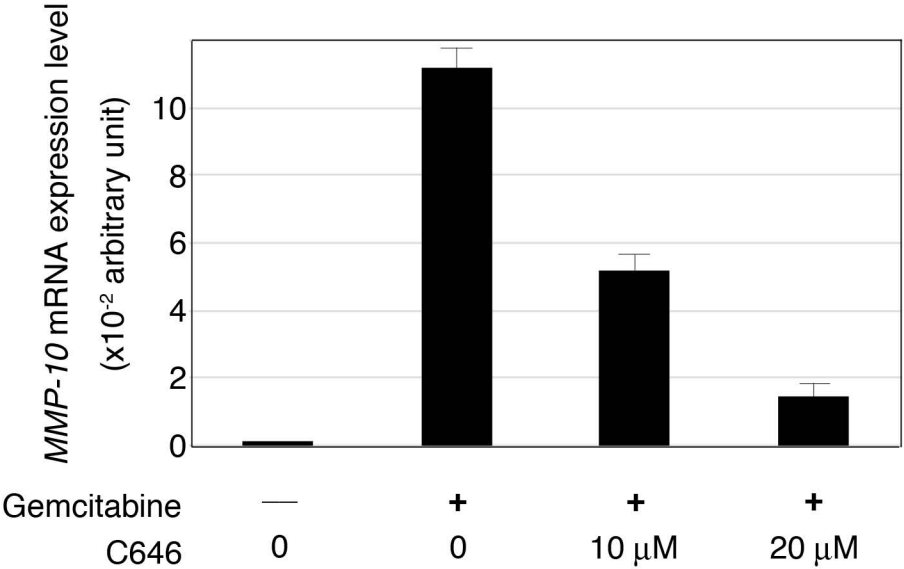
B



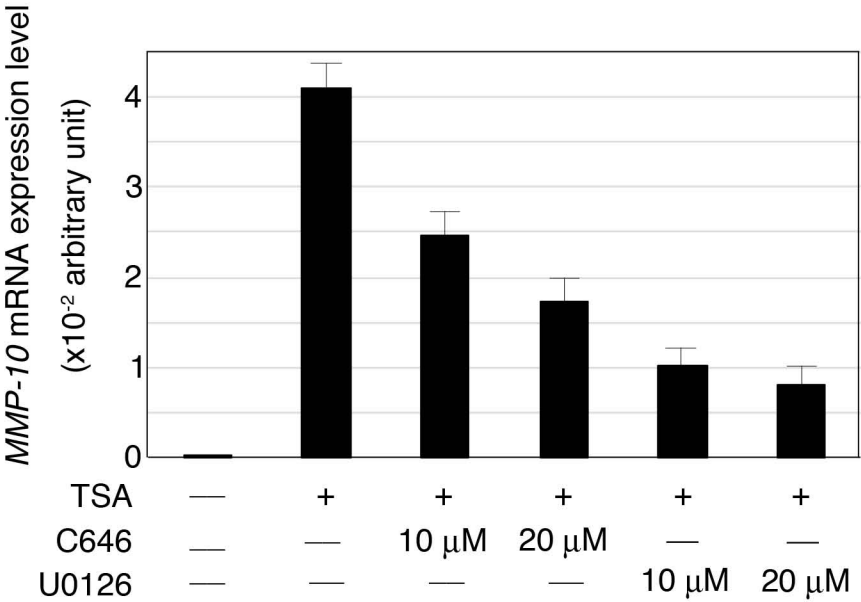
C



A



B



C

